Water **2015**, *7*, 5910-5927; doi:10.3390/w7115910

OPEN ACCESS

water

ISSN 2073-4441
www.mdpi.com/journal/water

Article

Spatial and Temporal Correlates of Greenhouse Gas Diffusion from a Hydropower Reservoir in the Southern United States

Jennifer J. Mosher [1,†,*], Allison M. Fortner [1], Jana R. Phillips [1], Mark S. Bevelhimer [1], Arthur J. Stewart [2,‡] and Matthew J. Troia [1]

[1] Oak Ridge National Laboratory Environmental Sciences Division, P.O. Box 2008, Oak Ridge, TN 37831-6351, USA; E-Mails: fortneram@ornl.gov (A.M.F.); randolphjd1@ornl.gov (J.R.P.); bevelhimerms@ornl.gov (M.S.B.); troiamj@ornl.gov (M.J.T.)

[2] Xcel Engineering Inc., 1066 Commerce Park Drive, Oak Ridge, TN 37830-0117, USA; E-Mail: stewartaj@ornl.gov

[†] Present address: Department of Biological Sciences, Marshall University, 1 John Marshall Drive, Huntington, WV 25755-2510, USA.

[‡] Present address: Science Education Program, Oak Ridge Associated Universities, P.O. Box 117, MS 36, Oak Ridge, TN 37831-0117, USA.

* Author to whom correspondence should be addressed; E-Mail: Mosher@marshall.edu; Tel.: +1-304-696-3637; Fax: +1-304-696-7186.

Academic Editor: Miklas Scholz

Received: 25 August 2015 / Accepted: 21 October 2015 / Published: 29 October 2015

Abstract: Emissions of CO_2 and CH_4 from freshwater reservoirs constitute a globally significant source of atmospheric greenhouse gases (GHGs), but knowledge gaps remain with regard to spatiotemporal drivers of emissions. We document the spatial and seasonal variation in surface diffusion of CO_2 and CH_4 from Douglas Lake, a hydropower reservoir in Tennessee, USA. Monthly estimates across 13 reservoir sites from January to November 2010 indicated that surface diffusions ranged from 236 to 18,806 $mg \cdot m^{-2} \cdot day^{-1}$ for CO_2 and 0 to 0.95 $mg \cdot m^{-2} \cdot day^{-1}$ for CH_4. Next, we developed statistical models using spatial and physicochemical variables to predict surface diffusions of CO_2 and CH_4. Models explained 22.7% and 20.9% of the variation in CO_2 and CH_4 diffusions respectively, and identified pH, temperature, dissolved oxygen, and Julian day as the most informative predictors. These findings provide baseline estimates of GHG emissions from a reservoir in eastern temperate North America, a region for which estimates of reservoir GHGs

emissions are limited. Our statistical models effectively characterized non-linear and threshold relationships between physicochemical predictors and GHG emissions. Further refinement of such modeling approaches will aid in predicting current GHG emissions from unsampled reservoirs and forecasting future GHG emissions.

Keywords: climate change; CH_4; CO_2; hydropower; random forests model; reservoir

1. Introduction

Hydropower is an important renewable component of national energy portfolios in many countries. Although hydropower traditionally has been considered to be carbon neutral [1], recent investigations suggest that the reservoirs created by large hydropower dams emit greenhouse gases (GHG), primarily carbon dioxide (CO_2), methane (CH_4), and nitrous oxide (N_2O) [2,3]. For example, Barros *et al.* [4] estimated that hydropower reservoirs release to the atmosphere 48 Tg of carbon as CO_2 and 3 Tg of carbon as CH_4 each year, based on extrapolation of emissions estimates from 85 globally distributed hydropower reservoirs. This carbon emission rate comprises 4% of the total net carbon emitted from the surfaces of all natural and human-created freshwater bodies and therefore represents a significant component of the global carbon cycle [4]. Emissions of GHGs from reservoirs occur via three main pathways. First, accumulation of dissolved GHGs in the water column, primarily originating from microbial metabolism, leads to passive diffusion from the reservoir surface to the atmosphere [2,5]. Second, gas bubble ebullition from the sediments of the reservoir also contribute to GHG emissions, particularly in the form CH_4 from shallow areas of reservoirs [6–9]. More recent investigations have documented the ebullition of microbubbles generated from oxic production of CH_4 in the water column is also a source of GHG emission from reservoirs [10]. Third, the rapid decrease in pressure as water leaves the reservoir, passes through the hydroelectric turbine, and is expelled into the tailrace allows GHGs to diffuse into the atmosphere. The relative contribution of GHGs from these three pathways varies from reservoir to reservoir and across seasons, and depends on various factors related to reservoir morphometry, age, and dam operation [3,4,11]. Nevertheless, surface diffusion often is the dominant contributor of GHG emissions [3,8,11], and is the focus of this study.

Many environmental factors contribute to the spatial and temporal variation in GHG surface diffusion. From a spatial perspective, surface diffusion of GHGs varies among reservoirs distributed along broad geographic gradients. For example, mean annual air temperature is a key factor affecting GHG emissions, with low-latitude tropical reservoirs typically emitting GHGs at greater rates per unit area than high-latitude temperate and boreal reservoirs [4]. Additionally, nutrient loading from the upstream catchment also contributes to variation in GHG emissions among reservoirs receiving drainage from agricultural *versus* natural land cover [3]. Emissions of GHGs also vary along environmental gradients within reservoirs. For example, ebullition occurs most often in shallow areas where bubbles remain intact. Bubbles originating from deeper areas can dissolve in the water column before reaching the reservoir surface resulting in greater passive diffusion [6–8,12]. Longitudinal position within the reservoir is also important, with shallow river delta habitats in the upper reservoir typically producing more GHGs than deeper reservoir habitats nearer the dam [3]. From a temporal

perspective, GHG emissions vary among years and among seasons within a year. Emissions of GHGs correlate negatively with reservoir age because new reservoirs generally contain larger pools of labile organic carbon from inundated terrestrial vegetation relative to older reservoirs [13]. Emissions of GHGs also vary within a year due to seasonal changes in temperature, nutrient availability, hydrology, and stratification-turnover dynamics [3,14].

Identifying the spatial and temporal drivers of GHG emissions within and among reservoirs is an important step in developing a predictive framework that can be used to forecast future GHG emissions of existing reservoirs as well as those reservoirs currently under construction or planned for construction. The ability to identify environmental correlates of GHG emissions requires data on GHG emissions from environments and geographic regions that have not previously been studied. In particular, many of the investigations of GHG emissions by reservoirs have taken place in tropical or boreal regions [4,15]. Fewer studies have been undertaken in reservoirs at mid-latitudes (but see [3,16,17]) even though approximately 30% of all reservoirs occur at these latitudes throughout the world [4]. Also lacking are studies of seasonal variation in GHG emissions along environmental gradients within a single reservoir (but see [3]) [12].

The overall objective of this study was to evaluate spatial and temporal variation in GHG emissions from Douglas Lake, a hydropower reservoir in the southeastern United States. First, we measured fluxes of CO_2 and CH_4 from the reservoir to the atmosphere via surface diffusion. Measurements were made across seasons and throughout the reservoir to document spatial and temporal variation in diffusion rates. Second, we developed statistical models to quantitatively characterize environmental correlates of CO_2 and CH_4 surface diffusion in both space and time. To do this, we used a recently-developed statistical algorithm, Random Forests [18], which can identify non-linear and threshold relationships between predictor variables and the response variable. By developing statistical models, our goal was to elucidate environmental drivers of variation in CO_2 and CH_4 emissions within a reservoir. Such statistical models can be used to predict GHG emissions in other unsampled reservoirs in this geographic region, and possibly forecast GHG emissions following future environmental changes such as increased nutrient loading or rising air temperatures.

2. Materials and Methods

2.1. Study Site and Field Sampling

Douglas Lake is located in eastern Tennessee and was formed in 1943 following the construction of Douglas Dam on the French Broad River in the upper Tennessee River basin (Figure 1). Douglas Dam is 61 m in height and 520 m wide and is equipped with four Francis-type hydropower turbines with a total electricity generation capacity of 111 megawatts. Douglas Lake covers 115 km^2 and is managed by the Tennessee Valley Authority (TVA) primarily for flood storage and hydroelectric generation, but it is also used extensively for recreational activities [19]. The reservoir is a warm monomictic system and pool elevation fluctuates seasonally by approximately 13.4 m, with maximum drawdown occurring from December through February. Water quality deficiencies include low concentrations of dissolved oxygen, particularly in the hypolimnion during summer stratification [20].

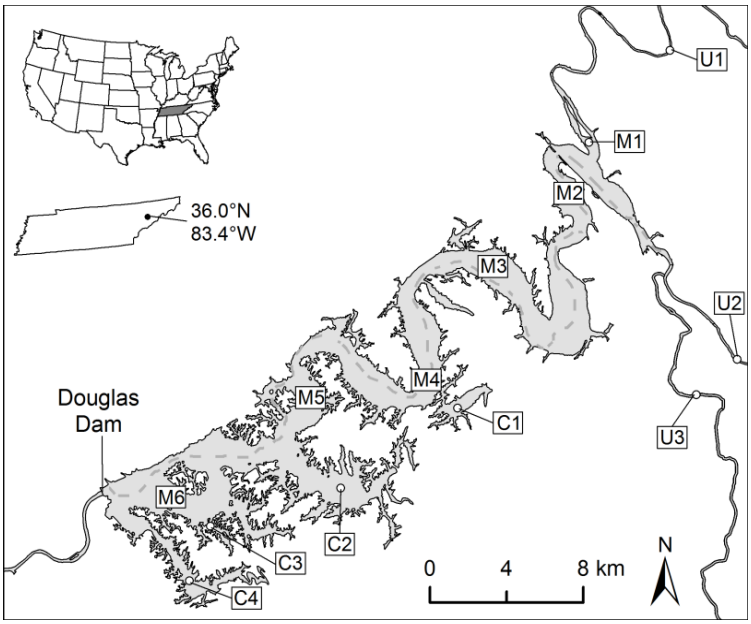

Figure 1. Locations of 13 study sites on Douglas Lake in eastern Tennessee, USA where CO_2 and CH_4 emissions and physicochemical variables were measured monthly from January through November 2010 (except February). Sites were distributed among lotic upstream (U1–U3), lentic main lake (M1–M6), and lentic cove (C1–C4) locations.

Field measurements were made monthly at 13 sites from January to November 2010, excluding February (Figure 1). During each monthly sampling campaign, all 13 sites were sampled over four or fewer consecutive days between the hours of 800 and 1800. Sites were distributed among six lentic main lake locations within Douglas Lake placed at increasing distances from Douglas Dam (M1–M6); four lentic cove locations within Douglas Lake placed at increasing distances from Douglas Dam (C1–C4), and three lotic locations on the Nolichucky River (U1), French Broad River (U2), and Pigeon River (U3) upstream of Douglas Lake. This distribution of sites captured spatial variation in environmental characteristics known to affect GHG production and surface diffusion [3,9,12].

2.2. CO_2 and CH_4 Emissions and Physicochemical Variables

We estimated CO_2 and CH_4 emissions using the thin boundary layer (TBL) method following a standard protocol outlined by the International Hydropower Association [20]. This method uses GHG concentration gradients at the water surface and semi-empirical equations to indirectly estimate GHG flux. Greenhouse gas diffusion estimates using the TBL method can be less accurate under certain conditions than direct measurement of diffusion using floating chambers [21], but still can provide useful estimates of GHG diffusion, particularly when a large number of locations and/or open windy lake locations are sampled [22]. Water samples were collected from within 0.5 m of the reservoir surface in 125-mL serum bottles sealed with butyl stoppers and preserved with potassium chloride (KCl). Samples were returned to the laboratory where headspace gas chromatography was used to measure the concentrations of dissolved CO_2 and CH_4 [23]. Two or three water samples were collected from each site on each sampling date, and the mean concentrations of gases in these subsamples were calculated and used in the following TBL calculations to estimate surface diffusions.

Gas diffusion from the water surface to the atmosphere can be estimated as the product of the concentration gradient between the surface water and air and a gas exchange coefficient (k) for CO_2 (Equation (1)) and CH_4 (Equation (2)).

$$CO_2 \text{ diffusion} = (\text{water}[CO_2] - \text{air}[CO_2]) \times k_{CO_2} \quad (1)$$

$$CH_4 \text{ diffusion} = (\text{water}[CH_4] - \text{air}[CH_4]) \times k_{CH_4} \quad (2)$$

Greenhouse gas concentrations from the water surface were calculated as the partial pressure of the gas (CO_2 or CH_4), which require data on water salinity, water temperature, air temperature, and atmospheric pressure. Gas exchange coefficients were calculated using the Schmidt number for each gas (CO_2 or CH_4), wind speed, and temperature. Air and water temperatures were measured at each site when water samples were collected. Wind velocity and atmospheric pressure measurements were acquired from a National Oceanic and Atmospheric Administration weather station located 34 km east of Douglas Dam [24]. Concentrations of CO_2 and CH_4 in the atmosphere were assumed to be 388 ppm and 1.8 ppm, respectively, based on recent global estimates [25]. We calculated monthly estimates of reservoir-wide diffusion of CO_2 and CH_4 by multiplying reservoir surface area (115 km^2) by the area-specific diffusion rates averaged across the ten lentic sites (M1–M6 and C1–C4). These reservoir-wide estimates assume that the ten lentic sampling locations capture the spatial variation in CO_2 and CH_4 surface diffusion; this method has been used in previous estimates of reservoir-wide GHG emissions [3].

In addition to GHG emissions, measurements of temperature, dissolved oxygen (O_2), conductivity, and pH were made from the surface and bottom of the water column on each sampling date from each site using a multiparameter data sonde (Model 6820 V2; YSI Inc.; Yellow Springs, OH, USA). Additional water samples were collected from the surface and bottom of the water column on each sampling date from each site using a van Dorn water sampler; then samples were analyzed for dissolved organic carbon (DOC), ammonium (NH_4^+), nitrate (NO_3^-), soluble reactive phosphorus (SRP), and total phosphorus (TP) concentrations using standard methods [18].

2.3. Data Analysis

We calculated sample averages and 95% confidence intervals for surface and bottom values of physicochemical variables and surface concentrations of CO_2 and CH_4 for each month (sites pooled) and for each site (months pooled) to summarize the spatial and temporal variation in GHG flux from Douglas Lake. We also calculated sample averages and 95% confidence intervals for surface concentrations and diffusive fluxes of CO_2 and CH_4 for each month (sites pooled) and for each site (months pooled) to summarize and visualize the spatial and temporal variation in GHG flux from Douglas Lake.

We developed statistical models to identify environmental correlates of CO_2 and CH_4 surface diffusions across the reservoir and among seasons. The Random Forests algorithm generates a regression tree using a random subset of the observations (*i.e.*, samples) and environmental predictor variables. This procedure is repeated many times (*i.e.*, 1000 times for the present analysis) and the response variable is predicted using a composite of all regression trees (*i.e.*, the forest). This recently-developed statistical algorithm is useful for characterizing nonlinear relationships between predictor variables and the response variable, modeling high order and complex interactions among predictor variables, and

accommodating missing values of predictor variables [26]. These properties make Random Forests models more accurate and informative than more traditional techniques (e.g., multiple linear regression) when modeling complex ecological responses [26]. We screened a total of 23 environmental predictor variables measured during field sampling for use as predictors in the random forest models. We calculated pairwise correlation coefficients of all 23 variables and removed highly correlated ($R > 0.7$) variables, retaining the variable from each pair that was hypothesized to be more causally linked to GHG fluxes (e.g., SRP instead of TP). We also removed CO_2 and CH_4 concentrations, wind speed, and surface water temperature because these variables are used directly in the TBL equations and would artificially inflate model performance if included as predictors. Sixteen variables were retained as predictors in the Random Forests models (Table 1). These variables were used to develop separate models for CO_2 and CH_4. Model performance was evaluated as the percent of variance explained, and statistical significance was evaluated by testing for linear relationships between model-predicted and observed GHG fluxes. We quantified the importance of predictor variables as the decrease in node impurity standardized from zero to one [26]. Lastly, we created partial dependence plots to visualize the independent effects of each of the five most important predictor variables for the CO_2 and CH_4. Partial dependence plots are useful for identifying non-linear or threshold relationships between predictors and the response. Because Random Forests models are a composite of many separate regression trees built from a random subset of the predictors, partial dependence plots can effectively display the relationship between the response and a single predictor variable, while factoring out the effects of the remaining predictor variables [26]. Statistical analyses were performed in the R programming environment using the randomForest library [27].

Table 1. Importance of 16 environmental predictor variables in explaining variation in surface diffusion of CO_2 and CH_4 based on thin boundary layer (TBL) estimation at six lentic main lake sites (M1–M6), four lentic cove sites (C1–C4), and three upstream lotic sites (U1–U3). Variable importance was measured as the decrease in node impurity of each Random Forests model with values standardized from 0 to 1.

Predictor	CO_2	CH_4
Julian day	0.49	0.35
Longitudinal position	0.33	0.01
Depth	0.06	0
O_2 bottom concentration	0	0.12
DOC bottom concentration	0.39	0.17
NH_4^+ bottom concentration	0.29	0.11
NO_3^- bottom concentration	0.11	0.07
pH bottom	0.2	0.05
SRP bottom	0.03	0.16
Temperature bottom	0.08	1
O2 surface concentration	0.28	0.83
DOC surface concentration	0.3	0.36
NH_4^+ surface concentration	0.01	0.03
NO_3^- surface concentration	0.27	0.11
pH surface	1	0.59
SRP surface	0.13	0.17

3. Results and Discussion

3.1. Physicochemical Conditions of Douglas Lake

Physicochemical factors (averaged across seasons) varied across sampling sites at Douglas Lake (Table 2). Main lake sampling sites increased in depth from a seasonal average of 2.5 m in the upstream-most site (M1) to 25.2 m in the downstream-most site (M6). Upstream lentic sites were the shallowest (~1.5 m) and cove sites were of moderate depths, ranging from 4.8 to 15.7 m. Surface temperatures averaged across seasons were generally consistent across sites, ranging from 20.7 °C to 27.6 °C. Bottom temperatures averaged across seasons were lowest in the deep downstream-most site (M6). Likewise, O_2 concentrations at the surface were consistently high across sites (7.4 to 10.0 $mg \cdot L^{-1}$), whereas bottom O_2 concentrations varied across sites (3.1 to 8.9 $mg \cdot L^{-1}$) and were lowest in the downstream-most main lake sites due to thermal stratification during the summer. DOC concentrations were consistent across sites at the surface (2.1 to 4.9 $mg \cdot L^{-1}$), but were more variable across sites at the bottom (1.7 to 6.9 $mg \cdot L^{-1}$). Concentrations of NH_4^+, NO_3^-, SRP, and TP as well as pH varied across sites, but did not show consistent upstream-to-downstream, lentic-to-lotic, or main lake-to-cove trends.

Physicochemical factors (averaged across sites) varied seasonally (Table 3). Depth at all sites except the lotic upstream sites peaked in the spring, declined steadily through the summer, and were lowest in the winter due to management of pool elevation by the TVA. Mean monthly surface temperatures ranged from 3.2 °C in January to 29.6 °C in July. Bottom temperatures showed a similar seasonal trend, but the maximum temperature in August (25.7 °C) was lower than surface temperature during that month due to thermal stratification. Concentrations of O_2 at the surface ranged from 7.5 $mg \cdot L^{-1}$ in August to 12.7 $mg \cdot L^{-1}$ in March. At the bottom of the water column, O_2 concentrations ranged from 3.0 $mg \cdot L^{-1}$ in August to 12.9 $mg \cdot L^{-1}$ in March. DOC at the surface and at the bottom ranged from 1.3 to 3.6 $mg \cdot L^{-1}$ from January to September, but were higher in October and November (range of 6.8 to 7.1 $mg \cdot L^{-1}$). Surface NH_4^+ concentrations ranged from 13.1 to 50.1 $\mu g\ N \cdot L^{-1}$ across months, but did not exhibit noticeable seasonal cycles. Bottom NH_4^+ concentrations, bottom and surface concentrations of $NO3^-$, and bottom and surface concentrations of SRP were variable across months but did not exhibit noticeable seasonal cycles.

Table 2. Spatial variation in physicochemical variables of Douglas Lake. Values are sample averages with 95% confidence intervals in parentheses. Confidence intervals for sample averages represented by a single sample (*i.e.*, no seasonal replication) are denoted with NAs.

Variable	M1	M2	M3	M4	M5	M6	C1	C2	C3	C4	U1	U2	U3
Depth (m)	2.5 (0.3)	7.9 (1.5)	9.5 (2.3)	11.8 (2.3)	20.0 (3.3)	25.2 (2.5)	10.1 (2.4)	15.7 (1.6)	4.8 (1.9)	11.8 (2.7)	1.5 (NA)	1.5 (NA)	1.5 (NA)
Surface temperature (°C)	27.6 (2.3)	27.6 (1.9)	23.6 (4.9)	23.2 (5.0)	23.1 (4.7)	20.7 (5.9)	23.0 (5.1)	23.0 (4.8)	20.8 (5.6)	22.0 (6.4)	23.7 (4.4)	20.9 (4.6)	20.3 (3.8)
Bottom temperature (°C)	26.7 (2.8)	24.8 (1.4)	20.3 (4.3)	19.8 (3.6)	16.7 (4.1)	14.5 (4.2)	19.0 (4.5)	18.9 (4.7)	20.1 (5.4)	17.9 (5.0)	23.7 (4.4)	20.9 (4.6)	20.3 (3.8)
Surface O_2 ($mg \cdot L^{-1}$)	7.4 (1.4)	7.9 (1.0)	10.0 (1.5)	9.6 (1.0)	9.5 (1.3)	9.5 (1.4)	9.6 (1.5)	9.5 (1.5)	9.7 (1.5)	10.0 (1.9)	8.9 (1.5)	8.6 (0.9)	8.8 (0.9)
Bottom O_2 ($mg \cdot L^{-1}$)	6.8 (0.6)	5.0 (2.4)	4.0 (2.8)	3.1 (2.2)	4.8 (2.7)	4.1 (2.5)	4.6 (3.1)	5.6 (2.5)	8.8 (2.1)	5.9 (3.4)	8.9 (1.5)	8.6 (0.9)	8.8 (0.9)
Surface pH	8.16 (NA)	8.06 (0.44)	8.55 (0.42)	8.47 (0.45)	8.46 (0.48)	8.00 (0.31)	8.63 (0.22)	8.37 (0.54)	7.96 (0.29)	8.33 (0.36)	8.27 (0.43)	7.96 (0.43)	8.2 (0.35)
Bottom pH	8.13 (NA)	7.61 (0.31)	7.63 (0.25)	7.33 (0.42)	7.44 (0.28)	7.28 (0.20)	7.81 (0.36)	8.07 (0.26)	7.88 (0.17)	7.81 (0.37)	8.27 (0.43)	7.96 (0.43)	8.20 (0.35)
Surface DOC ($mg \cdot L^{-1}$)	2.1 (0.5)	2.6 (0.4)	2.8 (1.1)	3.3 (1.1)	3.0 (1.3)	2.8 (1.2)	3.4 (1.4)	3.1 (1.3)	2.9 (1.2)	2.7 (0.9)	4.6 (3.0)	3.4 (1.4)	4.9 (1.7)
Bottom DOC ($mg \cdot L^{-1}$)	2.3 (0.4)	2.5 (0.9)	4.3 (4.7)	4.0 (2.8)	6.7 (1.6)	1.7 (NA)	6.9 (NA)	5.0 (3.6)	1.8 (0.4)	5.8 (NA)	4.6 (3.0)	3.4 (1.4)	4.9 (1.7)
Surface NH_4^+ ($\mu g\ N \cdot L^{-1}$)	43.3 (20.5)	78.3 (64.9)	29 (18.3)	22.2 (12.0)	11.7 (8.5)	17.5 (10.1)	27.2 (13.5)	14.1 (7.7)	24.9 (14.4)	18.8 (12.1)	21.7 (12.8)	20.5 (20.9)	15.7 (7.4)
Bottom NH_4^+ ($\mu g\ N \cdot L^{-1}$)	46.3 (19.5)	327.0 (348.2)	447.7 (352.1)	406.0 (331.7)	338.3 (603.5)	57.6 (NA)	81.5 (NA)	26.7 (22.7)	23.3 (14.6)	12.0 (NA)	21.7 (12.8)	20.5 (20.9)	15.7 (7.4)
Surface NO_3^- ($\mu g\ N \cdot L^{-1}$)	241.4 (112.4)	356.8 (236.9)	110.7 (100.2)	108.3 (81.7)	111.7 (90.2)	169.6 (119.3)	77.7 (65.4)	176.1 (118.3)	174.6 (119.1)	176.1 (126.9)	357.3 (126.5)	536.2 (122.0)	356.4 (78.6)
Bottom NO_3^- ($\mu g\ N \cdot L^{-1}$)	251.9 (138.4)	485.9 (137.1)	222.0 (370.5)	261.4 (197.8)	138.4 (80.2)	47.8 (NA)	70.1 (NA)	220.5 (127.6)	112.1 (171.4)	62.0 (NA)	357.3 (126.5)	536.2 (122.0)	356.4 (78.6)
Surface SRP ($\mu g\ P \cdot L^{-1}$)	17.1 (10.7)	33.5 (25.1)	11.5 (4.3)	9.2 (3.7)	6.1 (3.1)	7.8 (2.9)	7.6 (3.3)	4.5 (2.2)	6.9 (2.5)	6.6 (3.3)	28.6 (18.7)	36.3 (14.6)	25.5 (16.2)
Bottom SRP ($\mu g\ P \cdot L^{-1}$)	12.6 (11.4)	60.7 (24.9)	14.6 (2.1)	8.3 (2.2)	2.7 (3.1)	11.8 (NA)	1.0 (NA)	5.0 (4.4)	8.0 (4.1)	6.3 (NA)	28.6 (18.7)	36.3 (14.6)	25.5 (16.2)

Table 3. Seasonal variation in physicochemical variables of Douglas Lake. Values are sample averages with 95% confidence intervals in parentheses. Confidence intervals for sample averages represented by a single sample (*i.e.*, no spatial replication) are denoted with NAs.

Variable	January	February	March	April	May	June	July	August	September	October	November	December
Depth (m)	8.0	–	8.6	11.4	12	11.9	11.3	11.6	9.0	8.4	7.9	–
	(9.6)	–	(4.4)	(5.1)	(4.9)	(4.9)	(4.9)	(4.8)	(3.9)	(3.9)	(5.3)	–
Surface temperature (°C)	3.2	–	9.6	19.3	23.6	28.7	29.6	29.4	25.6	20.3	13.7	–
	(1.3)	–	(0.5)	(1.5)	(1.4)	(0.5)	(1.3)	(1.4)	(1.2)	(1.8)	(0.9)	–
Bottom temperature (°C)	3.4	–	7.5	14.6	19.6	23.0	24.7	25.7	24.6	19.8	12.8	–
	(1.2)	–	(1.4)	(1.8)	(1.9)	(2.8)	(1.9)	(2.1)	(1.1)	(1.7)	(0.8)	–
Surface O_2 ($mg \cdot L^{-1}$)	12.5	–	12.7	12.4	9.2	8.8	7.8	7.5	8.0	8.7	9.9	–
	(0.7)	–	(0.7)	(1.2)	(0.8)	(0.4)	(0.3)	(0.3)	(0.3)	(0.7)	(0.9)	–
Bottom O_2 ($mg \cdot L^{-1}$)	9.6	–	12.9	8.0	5.5	3.0	3.3	3.7	5.4	7.5	8.8	–
	(5.3)	–	(0.4)	(1.5)	(1.7)	(1.7)	(2.1)	(1.8)	(1.5)	(1.4)	(1.4)	–
Surface pH	7.7	–	8.11	9.51	–	–	7.69	8.42	8.33	8.2	8.34	–
	(0.36)	–	(0.32)	(0.04)	–	–	(0.19)	(0.27)	(0.21)	(0.19)	(0.25)	–
Bottom pH	7.63	–	7.95	7.56	–	–	7.69	7.46	7.73	8.02	8.04	–
	(0.38)	–	(0.22)	(0.64)	–	–	(0.19)	(0.3)	(0.18)	(0.26)	(0.34)	–
Surface DOC ($mg \cdot L^{-1}$)	1.7	–	1.6	2.3	2.2	2.4	3.2	2.6	2.2	6.8	7.0	–
	(0.4)	–	(0.3)	(0.4)	(0.2)	(0.2)	(0.9)	(0.4)	(0.4)	(0.9)	(1.1)	–
Bottom DOC ($mg \cdot L^{-1}$)	–	–	1.3	1.7	2.0	2.0	3.6	3.1	2.5	6.9	7.1	–
	–	–	(0.2)	(0.7)	(0.5)	(0.5)	(1.5)	(0.8)	(0.9)	(1.1)	(1.8)	–
Surface NH_4^+ ($\mu g\ N \cdot L^{-1}$)	50.1	–	27.9	41.3	24.9	16.3	30.6	26.4	15.9	13.1	13.9	–
	(21.9)	–	(6.4)	(14.8)	(10.5)	(5.6)	(31.0)	(15)	(6.1)	(12.4)	(8.1)	–
Bottom NH_4^+ ($\mu g\ N \cdot L^{-1}$)	–	–	23.4	14.5	25.4	155.6	124.4	47.9	32.8	164.6	232.3	–
	–	–	(NA)	(8.9)	(6.1)	(255.9)	(101.5)	(23.7)	(19.3)	(185.9)	(268.1)	–
Surface NO_3^- ($\mu g\ N \cdot L^{-1}$)	518.7	–	405.9	147.8	199.6	120.5	125.6	310.3	202.9	164.4	258.4	–
	(67.9)	–	(38.0)	(49.7)	(98.5)	(88.4)	(90.6)	(185.3)	(139.6)	(64.0)	(67.0)	–
Bottom NO_3^- ($\mu g\ N \cdot L^{-1}$)	–	–	445.5	269.3	438.2	283.3	253.6	519.2	366.6	175.5	325.8	–
	–	–	(28.5)	(62.8)	(57.7)	(122.5)	(137.3)	(286.4)	(218.0)	(101.9)	(96.1)	–
Surface SRP ($\mu g\ P \cdot L^{-1}$)	13.5	–	10.8	9.6	7.2	12.4	17.4	23.8	27.0	4.9	9.3	–
	(2.7)	–	(2.7)	(2.9)	(4.6)	(7.9)	(9.4)	(14.4)	(13.5)	(3.2)	(2.7)	–
Bottom SRP ($\mu g\ P \cdot L^{-1}$)	–	–	9.3	13.5	16.5	23.8	28.1	49.9	44.8	6.7	8.0	–
	–	–	(2.0)	(7.9)	(8.9)	(12.5)	(17.3)	(23.2)	(25.3)	(4.2)	(3.8)	–

Concentrations of CO_2 and CH_4 at the surface of the reservoir also exhibited seasonal and spatial trends (Figure 2). Averaged across seasons, CO_2 concentrations ranged from 103 μmol·L^{-1} at site C3 to 412 μmol·L^{-1} at site U3 and CH_4 concentrations ranged from 0.016 μmol·L^{-1} at site C2 to 0.089 μmol·L^{-1} at site M1 (Figure 2A,C). Averaged across sites, CO_2 concentrations ranged from 39.7 μmol·L^{-1} in October to 481.4 μmol·L^{-1} in March and CH_4 concentrations ranged from 0.003 μmol·L^{-1} in April to 0.132 μmol·L^{-1} in January (Figure 2B,D).

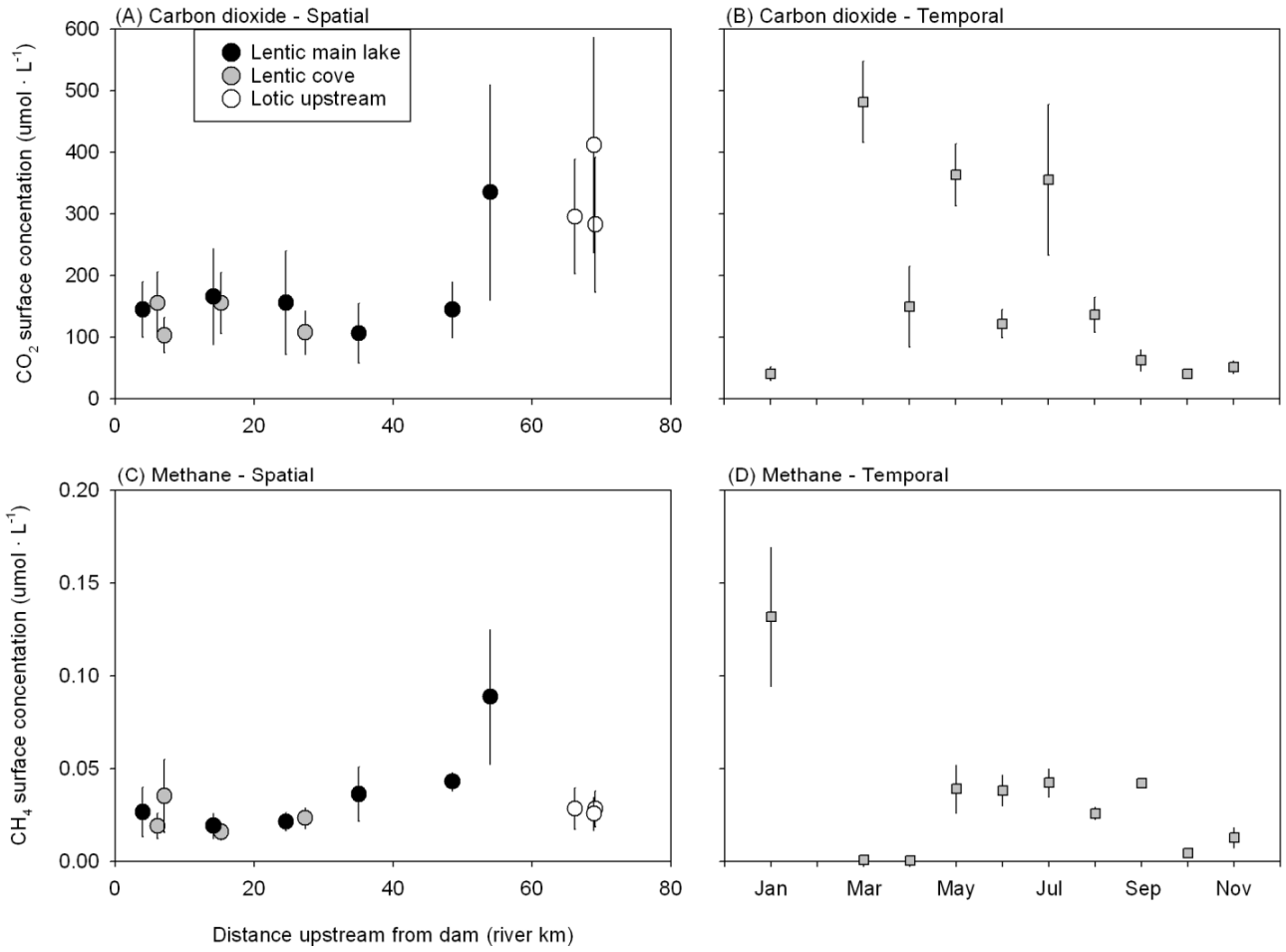

Figure 2. Surface concentrations of (**A**,**B**) CO_2 and (**C**,**D**) CH_4 from Douglas Lake as functions of (**A**,**C**) longitudinal position and (**B**,**D**) month of the year. Error bars represent 95% confidence intervals around the sample average.

3.2. CO_2 and CH_4 Emissions from Douglas Lake

Reservoir-wide estimates of surface diffusion ranged from 27,137 kg·day^{-1} in January to 2,091,331 kg·day^{-1} in July for CO_2 and 0 kg·day^{-1} in March and April to 71 kg·day^{-1} in July for CH_4. Area-specific rates of CO_2 surface diffusion varied spatially with the low rates ranging from 2480 to 6471 mg·m^{-2}·day^{-1} in the downstream-most main lake sites (M2–M6) and cove sites (C1–C4), whereas higher rates ranging from 12,177 to 18,806 mg·m^{-2}·day^{-1} occurred in the upstream-most lentic main lake site (M1) and the three upstream lotic sites (U1–U3) (Figure 3A). Area-specific rates of CH_4 surface diffusion also increased from downstream to upstream within the lentic main lake and cove sites, ranging from 0.25 mg·m^{-2}·day^{-1} at the downstream-most main lake site (M6) to

0.95 $mg \cdot m^{-2} \cdot day^{-1}$ at the upstream-most main lake site (M1). Surface diffusion of CH_4 declined precipitously between the main lake site located the furthest upstream (M1) and the lotic upstream sites (U1–U3) (Figure 3C). Surface diffusion rates of CO_2 and CH_4 showed similar patterns across seasons. Averaged across all sites, surface diffusion ranged from 236 $mg \cdot m^{-2} \cdot day^{-1}$ in January to 18,185 $mg \cdot m^{-2} \cdot day^{-1}$ in July for CO_2 and from 0 $mg \cdot m^{-2} \cdot day^{-1}$ in March and April to 0.62 $mg \cdot m^{-2} \cdot day^{-1}$ in July for CH_4 (Figure 3B,D).

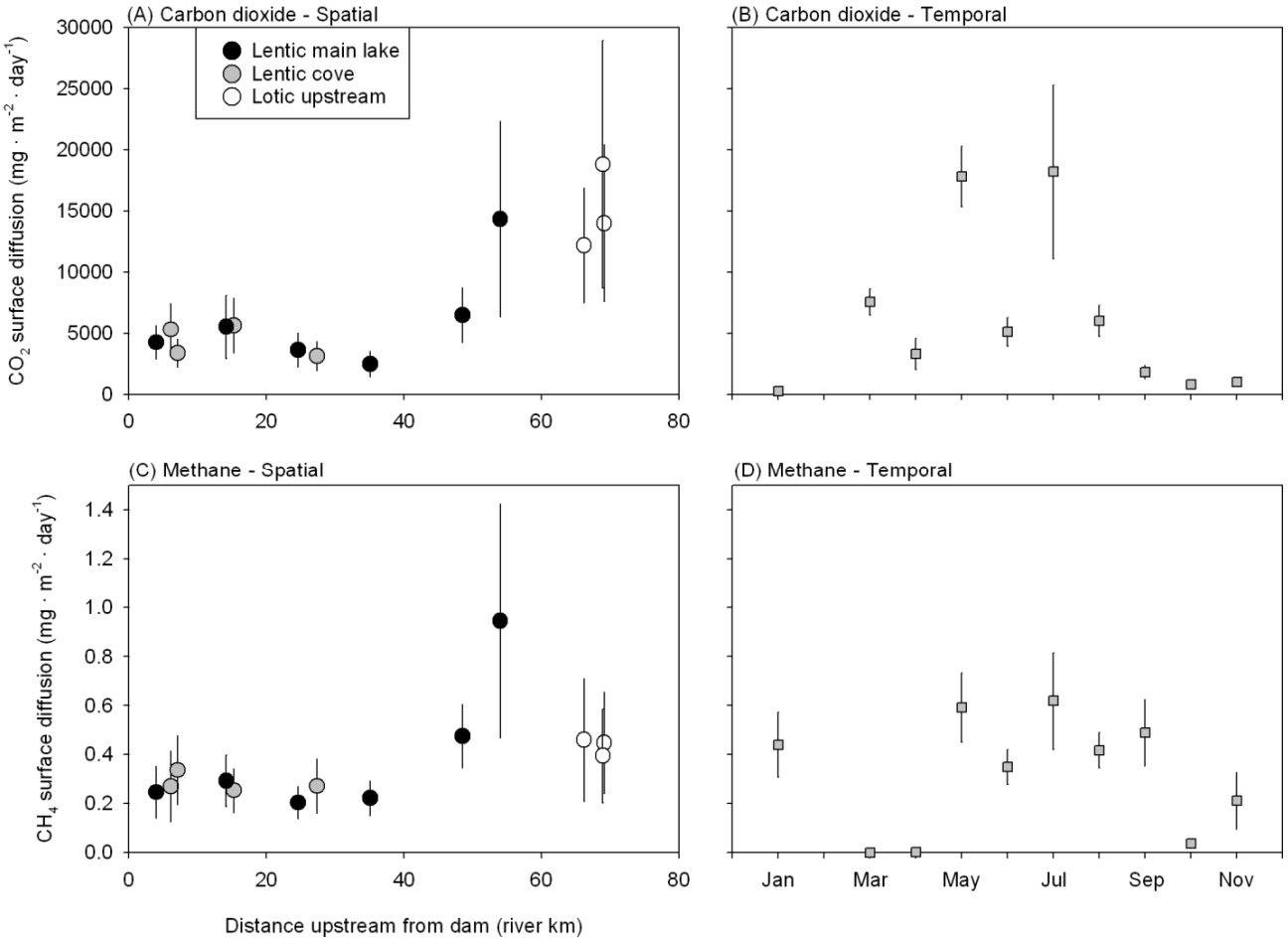

Figure 3. Surface diffusion of (**A**,**B**) CO_2 and (**C**,**D**) CH_4 from Douglas Lake as functions of (**A**,**C**) longitudinal position and (**B**,**D**) month of the year. Error bars represent 95% confidence intervals around the sample average.

Our evaluation of surface diffusion of CO_2 and CH_4 indicates that Douglas Lake is a net emitter of both of these GHGs, regardless of season or location within the reservoir. Emissions of CO_2 were four to five orders of magnitude greater than emissions of CH_4, which is consistent with previous studies of reservoir GHG emissions [11,22]. Our estimates of surface diffusion averaged across seasons and reservoir locations (7067 and 0.34 $mg \cdot m^{-2} \cdot day^{-1}$ for CO_2 and CH_4, respectively) fall within the range of previously reported rates of surface diffusion of these gases from other reservoirs throughout the world. Specifically, our estimates are similar to those from reservoirs in the Western United States [11], Canada [28–30], and Scandinavia [31], but are lower than estimates from tropical reservoirs [32]. These comparisons match the low-to-high latitude decline in GHG emissions reported by Barros *et al.* [4]. Only a few studies have reported GHG emissions from reservoirs in the eastern

United States. Beaulieu *et al.* [3] and Jacinthe *et al.* [33] reported higher emission rates, which could be a consequence of the higher agricultural land use (and consequent higher nutrient loading) surrounding their study reservoirs in Ohio and Indiana, respectively, compared to Douglas Lake.

Much recent research has focused on documenting among-reservoir variation in GHG emissions and identifying broad scale environmental drivers of this variation, such as latitude, net primary production, and reservoir morphology [4,11,34]. Less is known about environmental gradients driving variation in GHG emissions within a single reservoir. Our findings suggest that surface diffusion of CO_2 and CH_4 increases from downstream to upstream locations in the reservoir. This pattern has been documented in previous studies and has been attributed to shallow depths and greater nutrient and carbon availability from tributary influxes in upstream areas of the reservoir, particularly at the river delta [3]. Interestingly, we did not observe strong differences in GHG flux between deeper main lake and shallower cove locations located at similar longitudinal positions. This finding suggests that input of nutrients and labile carbon from the three major tributaries (Nolichucky, French Broad, and Pigeon Rivers), and not factors associated strictly with shallow water, is important in generating higher levels of GHG surface diffusion in shallow upstream areas.

Identifying seasonal variation in GHG emissions from hydropower reservoirs is also a key research need. We show that surface diffusion of CO_2 and CH_4 generally increases during the summer months, as observed in previous studies [22,31,32]. This pattern is consistent with higher temperatures throughout the water column and elevated rates of microbial metabolism, producing more CO_2 and CH_4 in bottom sediments and the water column [5,8,35]. Interestingly, we observed high surface concentrations and subsequent diffusion rates of CH_4 in January as well. This seasonal anomaly was apparent for the most downstream main lake and cove sites. Future work should focus on elucidating causes of this high CH_4 diffusion in January and exploring GHG fluxes in nearby reservoirs for similar seasonal anomalies.

3.3. Modelling Spatial and Temporal Variation in GHG Emissions

The Random Forests models were statistically significant ($p < 0.0001$) and explained 22.7% of the variance in CO_2 surface diffusion and 20.9% of the variance in CH_4 surface diffusion. Surface pH, Julian date, bottom DOC, distance upstream from the dam, and surface DOC were the five most important predictors of CO_2 diffusion, whereas bottom temperature, surface O_2, surface pH, surface DOC, and Julian date were the five most influential predictors of CH_4 diffusion (Table 1). Partial dependence plots revealed nonlinear relationships between environmental predictors and surface diffusions of CO_2 and CH_4 (Figure 4). Specifically, surface diffusion of CO_2 was highest when surface pH was less than eight and between Julian dates ranging from one to 180. Surface diffusion of CO_2 also increased notably between 40 and 70 km upstream from the dam. Surface diffusion of CH_4 was positively associated with bottom temperature, with diffusion increasing at temperatures of 25 °C and higher. Surface diffusion of CH_4 also declined notably when surface O_2 was above 7 $mg \cdot L^{-1}$ and when surface pH exceeded 7.5.

Multivariate statistical models have been applied to various questions related to global change biology [36,37], but they have had only limited application in studies of reservoir GHG emissions [4]. Our results suggest that multivariate statistical models can explain a moderate amount of variation

(20.9% to 22.7%) in CO_2 and CH_4 fluxes, using spatial factors and commonly-measured physicochemical factors as predictor variables. This lack of strong predictive capability could be due to several factors. First, we used TBL estimates of surface diffusion as the response variable, yet surface diffusion rates based on such estimates are inherently less accurate than direct measurements with floating chambers [21]. Second, diurnal cycling of CO_2 and CH_4 can influence rates of surface diffusion [5,38,39]; however, we did not include predictor variables to account for such diel variation. Third, although we included a variety of environmental variables as predictors, including other unmeasured environmental factors in statistical models would likely improve model performance. For example, structural and metabolic characteristics of lake-bottom sediments are known to be important drivers of GHG production and emissions in lakes and reservoirs [8,35]. Further, including temporally varying drivers such as tributary discharge and reservoir turnover rate would also likely improve model performance [3,10]. Nevertheless, relationships between GHG fluxes and the most influential predictor variables matched predictions based on known physicochemical properties as well as previous studies aimed at identifying environmental correlates of reservoir GHG emissions. For example, our partial dependence plots showed the negative relationship between CO_2 flux and surface pH expected due to the known relationship between CO_2 speciation and pH [5]. Other investigators have also noted a relationship between CO_2 flux and pH in reservoirs of the Western United States [10]. Likewise, CH_4 flux was positively associated with water temperature at the bottom of the reservoir and negatively associated with dissolved oxygen concentrations—factors that drive benthic microbial metabolism and anaerobic respiration pathways, respectively [5].

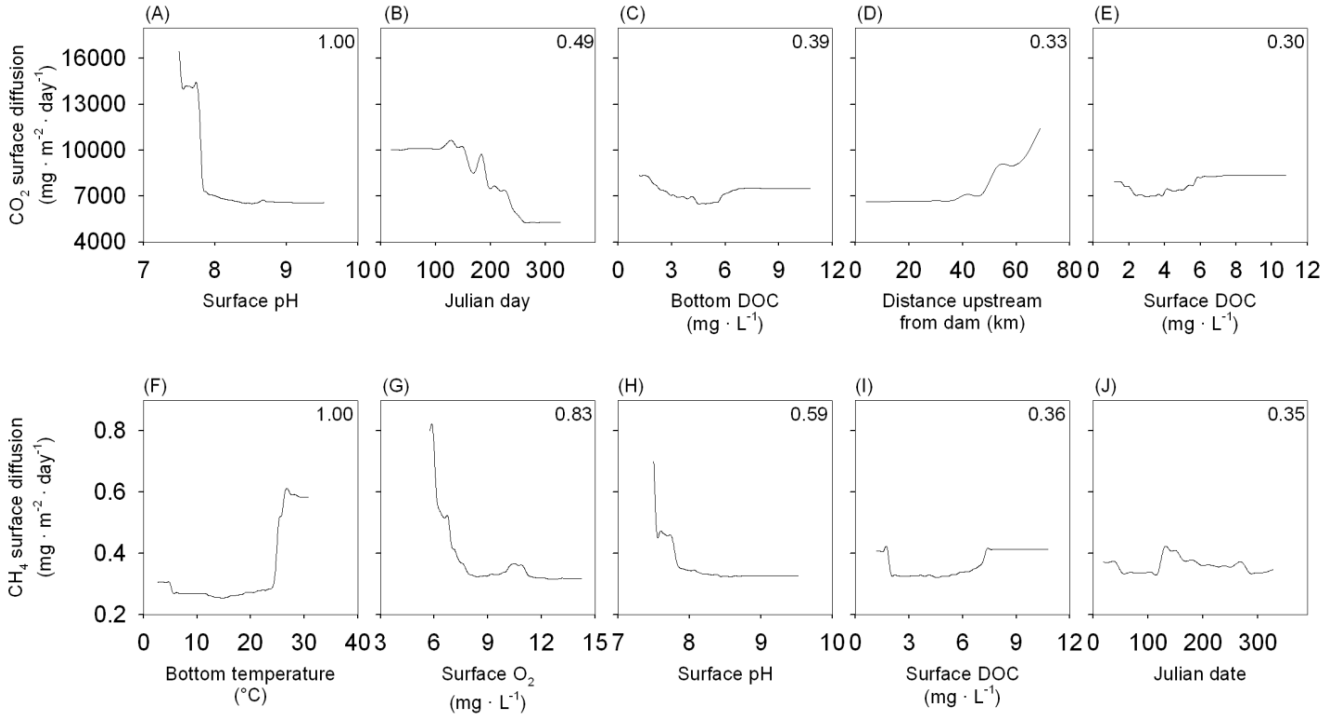

Figure 4. Partial dependence plots derived from Random Forests models showing the relationship between the five most influential environmental correlates (horizontal axes) and surface diffusion of (**A**,**B**) CO_2 and (**E**–**G**) CH_4. Inset numbers in each panel show variable importance. See Table 1 for a summary of variable importance for all 16 predictor variables.

Fundamental physicochemical relationships suggested by the results of our models indicate that our statistical models provide an essential first step toward developing and refining more precise and accurate statistical models which we view as an important goal in future studies of reservoir GHG emissions. In particular, further work should focus on measuring additional environmental variables that are hypothesized to be causally linked to GHG production in pelagic and benthic environments of the reservoir, as well as those variables linked to the flux of GHG via the key pathways. For example, sediment nutrient and oxygen conditions should be measured and used as causal predictors of CH_4 production and subsequent surface diffusion. Also, microbial abundance and functional composition in the pelagic zone in part determine the degree to which rising CH_4 bubbles are oxidized to CO_2 [14,38], and therefore may be precise and accurate predictors of CO_2 and CH_4 fluxes. Lastly, the use of recently developed and flexible statistical algorithms, such as Random Forests, allows investigators to identify nonlinear and threshold relationships between predictor and response, which is more informative than traditional correlative analyses based on linear regression [26].

Although our statistical models did not predict as precisely needed for the purpose of predicting or forecasting GHG emissions in other study systems, further refinement of statistical models like the ones we present here should be useful for several generally-applicable reasons. First, statistical models will improve understanding of cause-effect relationships between environmental and spatial factors and fluxes of GHGs. Second, models incorporating predictor variables compiled in a spatially continuous manner across a body of water (e.g., depth from digitized bathymetric maps) can be used to project GHG emissions in a spatially continuous manner. This approach can improve the precision of whole-reservoir emissions estimates over those estimates made from a small number of sampling stations placed in representative habitats and then extrapolated to the entire reservoir. Third, precise statistical models can be used to forecast emissions under future environmental conditions associated with reservoir aging [4] and/or changes in climate [40], nutrient loading [31], dam operations [3], or yet other unknown factors. Such models will be useful for life cycle analyses aimed at estimating the complete carbon footprint of hydropower projects starting with construction, extending through their operational lifetime, and ending with their decommissioning [34,41]. Lastly, although we developed a statistical model to predict spatial and seasonal variation in GHG emissions within a reservoir, this approach could easily be applied to broad-scale studies of variation in GHG emissions among reservoirs within a region, across a continent, or the entire globe. Such broad-scale studies will aid in better understanding broad scale drivers such as climate, reservoir type, or natural and human land cover. Estimates from such broad-scale studies will improve global estimates of GHG emissions from freshwater lakes and reservoirs necessary for understanding global carbon cycling and climate change. Moreover, forecasting among reservoir variation in GHG emissions can inform regional development of hydropower resources and provide estimates of cumulative GHG emissions from multiple reservoirs [42,43].

4. Conclusions

Although hydropower facilities are frequently viewed as a green source of energy, a growing body of literature suggests that GHG fluxes from their reservoirs contribute globally significant amounts of GHGs to the atmosphere [3,4,15]. The present study provides two important contributions. First, our findings provide baseline estimates of GHG emissions from a reservoir in temperate

North America—a region for which data are limited, despite having a relatively large number of hydropower-generating reservoirs. Second, we demonstrate the utility of statistical models as predictive tools for studying GHG emissions. Hydropower resources throughout the world are being developed rapidly, and additional development is planned. This development is particularly rapid in Asia and South America [44,45], but recent interest in expanding hydropower resource use in the United States and Canada is also being evaluated [46–49]. Deeper understanding and prediction of GHG flux within and among reservoirs is essential to forecast the potential impact of regional hydropower development scenarios [43] on the global carbon cycle and the consequent implications for anthropogenic climate change.

Acknowledgments

This manuscript is dedicated to the memory of our colleague, Pat Mulholland, who was instrumental in the conception and design of this project. This manuscript has been authored by UT-Battelle, LLC under Contract No. DE-AC05-00OR22725 with the US Department of Energy. The United States Government retains and the publisher, by accepting the article for publication, acknowledges that the United States Government retains a non-exclusive, paid-up, irrevocable, worldwide license to publish or reproduce the published form of this manuscript, or allow others to do so, for United States Government purposes. The Department of Energy will provide public access to these results of federally sponsored research in accordance with the DOE Public Access Plan (http://energy.gov/downloads/doe-public-access-plan). The research was supported by the United States Department of Energy's Office of Energy Efficiency and Renewable Energy, Wind and Water Power Technologies Program. We thank Natalie Griffiths, Brenda Pracheil, Glenn Cada, Walter Hill, and numerous anonymous reviewers for thoughtful and constructive comments on the manuscript, and Boualem Hadjerioua for providing data on Douglas Lake operations.

Author Contributions

Jennifer J. Mosher, Patrick J. Mulholland, and Mark S. Bevelhimer conceived and designed the study. Jennifer J. Mosher, Allison M. Fortner, and Jana R. Phillips collected the data. Matthew J. Troia analyzed the data. All authors wrote the paper.

Conflicts of Interest

The authors declare no conflict of interest.

References

1. Victor, D.G. Strategies for cutting carbon. *Nature* **1998**, *395*, 837–838.
2. Rudd, J.W.M.; Harris, R.; Kelly, C.A.; Hecky, R.E. Are hydroelectric reservoirs significant sources of greenhouse gases? *AMBIO* **1993**, *22*, 246–248.
3. Beaulieu, J.J.; Smolenski, R.L.; Nietch, C.T.; Townsend-Small, A.; Elovitz, M.S. High methane emissions from a midlatitude reservoir draining an agricultural watershed. *Environ. Sci. Technol.* **2014**, *48*, 11100–11108.

4. Barros, N.; Cole, J.J.; Tranvik, L.J.; Prairie, Y.T.; Bastviken, D.; Huszar, V.L.M.; del Giorgio, P.; Roland, F. Carbon emission from hydroelectric reservoirs linked to reservoir age and latitude. *Nat. Geosci.* **2011**, *4*, 593–596.
5. Wetzel, R.G. *Limnology: Lake and River Ecosystems*, 3rd ed.; Academic Press: San Diego, CA, USA, 2001.
6. Galy-Lacaux, C.; Delmas, R.; Jambert, C.; Dumestre, J.F.; Labroue, L.; Richard, S.; Gosse, P. Gaseous emissions and oxygen consumption in hydroelectric dams: A case study in French Guyana. *Glob. Biogeochem. Cycles* **1997**, *11*, 471–483.
7. McGinnis, D.F.; Greinert, J.; Artemov, Y.; Beaubien, S.E.; Wuest, A. Fate of rising methane bubbles in stratified waters: How much methane reaches the atmosphere? *J. Geophys. Res.* **2006**, *111*, doi:10.1029/2005JC003183.
8. Bastviken, D.; Cole, J.J.; Pace, M.L.; van de Bogert, M.C. Fates of CH_4 from different lake habitats: Connecting whole-lake budgets and CH_4 emissions. *J. Geophys. Res. Biogeosci.* **2008**, *113*, doi:10.1029/2007JG000608.
9. Delsontro, T.; Kunz, M.J.; Kempter, T.; Wuest, A.; Wehrli, B.; Senn, D.B. Spatial heterogeneity of methane ebullition in a large tropical reservoir. *Environ. Sci. Technol.* **2011**, *45*, 9866–9873.
10. Bogard, M.J.; del Giorgio, P.A.; Boutet, L.; Chaves, M.C.G.; Prairie, Y.T.; Merante, A.; Derry, A.M. Oxic water column methanogenesis as a major component of aquatic CH4 fluxes. *Nat. Commun.* **2014**, *5*, doi:10.1038/ncomms6350.
11. Soumis, N.; Duchemin, E.; Canuel, R.; Lucotte, M. Greenhouse gas emissions from reservoirs of the western United States. *Glob. Biogeochem. Cycles* **2004**, *18*, doi:10.1029/2003GB002197.
12. Hofmann, H. Spatiotemporal distribution patterns of dissolved methane in lakes: How accurate are the current estimations of the diffusive flux pathway? *Geophys. Res. Lett.* **2013**, *40*, 2779–2784.
13. Kelly, C.A.; Rudd, J.W.M.; Bodaly, R.A.; Roulet, N.P.; St. Louis, V.L.; Heyes, A.; Moore, T.R.; Schiff, S.; Aravena, R.; Scott, K.J.; *et al*. Increases in fluxes of greenhouse gases and methyl mercury following flooding of an experimental reservoir. *Environ. Sci. Technol.* **1997**, *31*, 1334–1344.
14. Kankaala, P.; Huotari, J.; Peltomaa, E.; Saloranta, T.; Ojala, A. Methanotrophic activity in relation to CH_4 efflux and total heterotrophic bacterial production in a stratified, humic, boreal lake. *Limnol. Oceanogr.* **2006**, *51*, 1195–1204.
15. St. Louis, V.; Kelly, C.A.; Duchemin, E.; Rudd, J.W.M.; Rosenberg, D.M. Reservoir surfaces as sources of greenhouse gases to the atmosphere: A global estimate. *BioScience* **2000**, *50*, 766–775.
16. DelSontro, T.; McGinnis, D.F.; Sobek, S.; Ostrovsky, I.; Wehrli, B. Extreme methane emissions from a Swiss hydropower reservoir: Contribution from bubbling sediments. *Environ. Sci. Technol.* **2010**, *44*, 2419–2425.
17. Maeck, A.; del Sontro, T.; McGinnis, D.F.; Fischer, H.; Flury, S.; Schmidt, M.; Fietzek, P.; Lorke, A. Sediment trapping by dams creates methane emission hot spots. *Environ. Sci. Technol.* **2013**, *47*, 8130–8137.
18. American Public Health Association. *Standard Methods for the Examination of Water and Wastewater*, 21st ed.; American Public Health Association: Washington, DC, USA, 2005.
19. Tennessee Valley Authority Website. Available online: http://www.tva.gov (accessed on 1 February 2015).

20. UNESCO/The International Hydropower Association. *GHG Measurement Guidelines for Freshwater Reservoirs*; Goldenfum, J.A., Ed.; London, UK, 2010.
21. Duchemin, E.; Lucotte, M.; Canuel, R. Comparison of static chamber and thin boundary layer equation methods for measuring greenhouse gas emissions from large water bodies. *Environ. Sci. Technol.* **1999**, *33*, 350–357.
22. Demarty, M.; Bastien, J.; Tremblay, A.; Hesslein, R.; Gill, R. Greenhouse gas emissions from boreal reservoirs in Manitoba and Quebec, Canada, measured with automated systems. *Environ. Sci. Technol.* **2009**, *43*, 8908–8915.
23. Ioffe, B.V.; Vitenberg, A.G. *Head-Space Analysis and Related Methods in Gas Chromotography*; Wiley: New York, NY, USA, 1984.
24. National Oceanic and Atmospheric Administration Website. Available online: http://www. noaa.gov (accessed on 1 February 2015).
25. Stocker, T.F.; Qin, D.; Plattner, G.K.; Tignor, M.; Allen, S.K.; Boschung, J.; Nauels, A.; Xia, Y.; Bex, V.; Midgley, P.M. (Eds.) Intergovernmental Panel on Climate Change. Summary for Policymakers. In *Climate Change 2013: The Physical Science Basis*; Contribution of Working Group I to the Fifth Assessment Report of the Intergovernmental Panel on Climate Change; Cambridge University Press: Cambridge, UK; New York, NY, USA, 2013.
26. Cutler, D.R.; Edwards, T.C.; Beard, K.H.; Cutler, A.; Hess, K.T.; Gibson, J.; Lawler, J.J. Random forests for classification in ecology. *Ecology* **2007**, *88*, 2783–2792.
27. Breiman, L.; Cutler, A. Random Forests. Available online: https://www.stat.berkeley.edu/~breiman/RandomForests/cc_home.htm (accessed on 2 April 2014).
28. Tremblay, A.; Lambert, M.; Gagnon, L. Do hydroelectric reservoirs emit greenhouse gases? *Environ. Manag.* **2004**, *33*, S509–S517.
29. Teodoru, C.R.; Prairie, Y.T.; del Giorgio, P.A. Spatial heterogeneity of surface CO_2 fluxes in a newly created Eastmain-1 Reservoir in Northern Quebec, Canada. *Ecosystems* **2011**, *14*, 28–46.
30. Tadonléké, R.D.; Marty, J.; Planas, D. Assessing factors underlying variation of CO_2 emissions in boreal lakes *vs.* reservoirs. *FEMS Microb. Ecol.* **2012**, *79*, 282–297.
31. Huttunen, J.T.; Alm, J.; Liikanen, A.; Juutinen, S.; Larmola, T.; Hammar, T.; Silvola, J.; Martikainen, P.J. Fluxes of methane, carbon dioxide and nitrous oxide in boreal lakes and potential anthropogenic effects on the aquatic greenhouse gas emissions. *Chemosphere* **2003**, *52*, 609–621.
32. Kemenes, A.; Forsberg, B.R.; Melack, J.M. CO_2 emissions from a tropical hydroelectric reservoir (Balbina, Brazil). *J. Geophys. Res.* **2011**, *116*, doi:10.1029/2010JG001465.
33. Jacinthe, P.A.; Filippelli, G.M.; Tedesco, L.P.; Raftis, R. Carbon storage and greenhouse gases emission from a fluvial reservoir in an agricultural landscape. *Catena* **2012**, *94*, 53–63.
34. Hertwich, E.G. Addressing Biogenic Greenhouse Gas Emissions from Hydropower in LCA. *Environ. Sci. Technol.* **2013**, *47*, 9604–9611.
35. West, W.E.; Coloso, J.J.; Jones, S.E. Effects of algal and terrestrial carbon on methane production rate and methanogen community structure in a temperature lake sediment. *Freshw. Biol.* **2012**, *57*, 949–955.
36. Guisan, A.; Thuiller, W. Predicting species distributions: Offering more than simple habitat models. *Ecol. Lett.* **2005**, *8*, 993–1009.

37. Tilman, D.; Fargione, J.; Wolff, B.; D'Antonio, C.; Dobson, A.; Howarth, R.; Schindler, D.; Schlesinger, W.J.; Simberloff, D.; Swackhamer, D. Forecasting agriculturally driven global environmental change. *Science* **2001**, *292*, 281–284.
38. Podgrajsek, E.; Sahlee, E.; Rutgersson, A. Diurnal cycle of lake methane flux. *J. Geophys. Res. Biogeosci.* **2014**, *119*, 236–248.
39. Grossart, H.P.; Frindte, K.; Dziallas, C.; Eckert, W.; Tang, K.W. Microbial methane production in oxygenated water column of an oligotrophic lake. *Proc. Natl. Acad. Sci. USA* **2011**, *108*, 19657–19661.
40. Tranvik, L.J.; Downing, J.A.; Cotner, J.B.; Loiselle, S.A.; Striegl, R.G.; Ballatore, T.J.; Dillon, P.; Finlay, K.; Fortino, K.; Knoll, L.B.; *et al*. Lakes and reservoirs as regulators of carbon cycling and climate. *Limnol. Oceanogr.* **2009**, *54*, 2298–2314.
41. Intergovernmental Panel on Climate Change. *IPCC Special Report on Renewable Energy Sources and Climate Change Mitigation*; Contribution of Working Group III to the Fifth Assessment Report of the Intergovernmental Panel on Climate Change; Edenhofer O., Pichs-Madruga, R., Sokona, Y., Seyboth, K., Matschoss, P., Kadner, S., Zwickel, T., Eickemeier, P., Hansen, G., Schlömer, S., *et al*., Eds.; Cambridge University Press: Cambridge, UK; New York, NY, USA, 2013; p. 1075.
42. Chang, X.; Liu, X.; Zhou, W. Hydropower in China at present and its further development. *Energy* **2010**, *35*, 4400–4406.
43. McManamay, R.A.; Samu, N.; Kao, S.C.; Bevelhimer, M.S.; Hetrick, S.C. A multi-scale spatial approach to address environmental effects of small hydropower development. *Environ. Manag.* **2014**, *55*, 217–243.
44. Mekong River Commission. *Economic, Environmental and Social Impact Assessment of Basin-Wide Water Resources Development Scenarios*; Mekong River Commission: Vientiane, Laos, 2009.
45. *Hydropower Policy*; Ministry of Power, Government of India (GOI): New Delhi, India, 2008.
46. Hadjerioua, B.Y.; Wei, Y.; Kao, S.C. *An Assessment of Energy Potential at Non-Powered Dams in the United States*; GPO DOE/EE-0711; Wind and Water Power Program, Department of Energy: Washington, DC, USA, 2012.
47. Kao, S.C.; McManamay, R.A.; Stewart, K.M.; Samu, N.M.; Hadjerioua, B.; DeNeale, S.T.; Yeasmin, D.; Pasha, M.F.K.; Oubeidillah, A.A.; Smith, B.T. *New Stream-Reach Development: A Comprehensive Assessment of Hydropower Energy Potential in the United States*; GPO DOE/EE-1063; Wind and Water Power Program, Department of Energy: Washington, DC, USA, 2014.
48. Canadian Hydropower Association. Report of Activities. Available online: http:// canadahydro.ca/ reportsreference/cha-reports-and-publications (accessed on 1 February 2015).
49. Hydropower in Canada: Past Present and Future. Available online: http://canadahydro.ca/ reportsreference/cha-reports-and-publications (accessed on 1 February 2015).